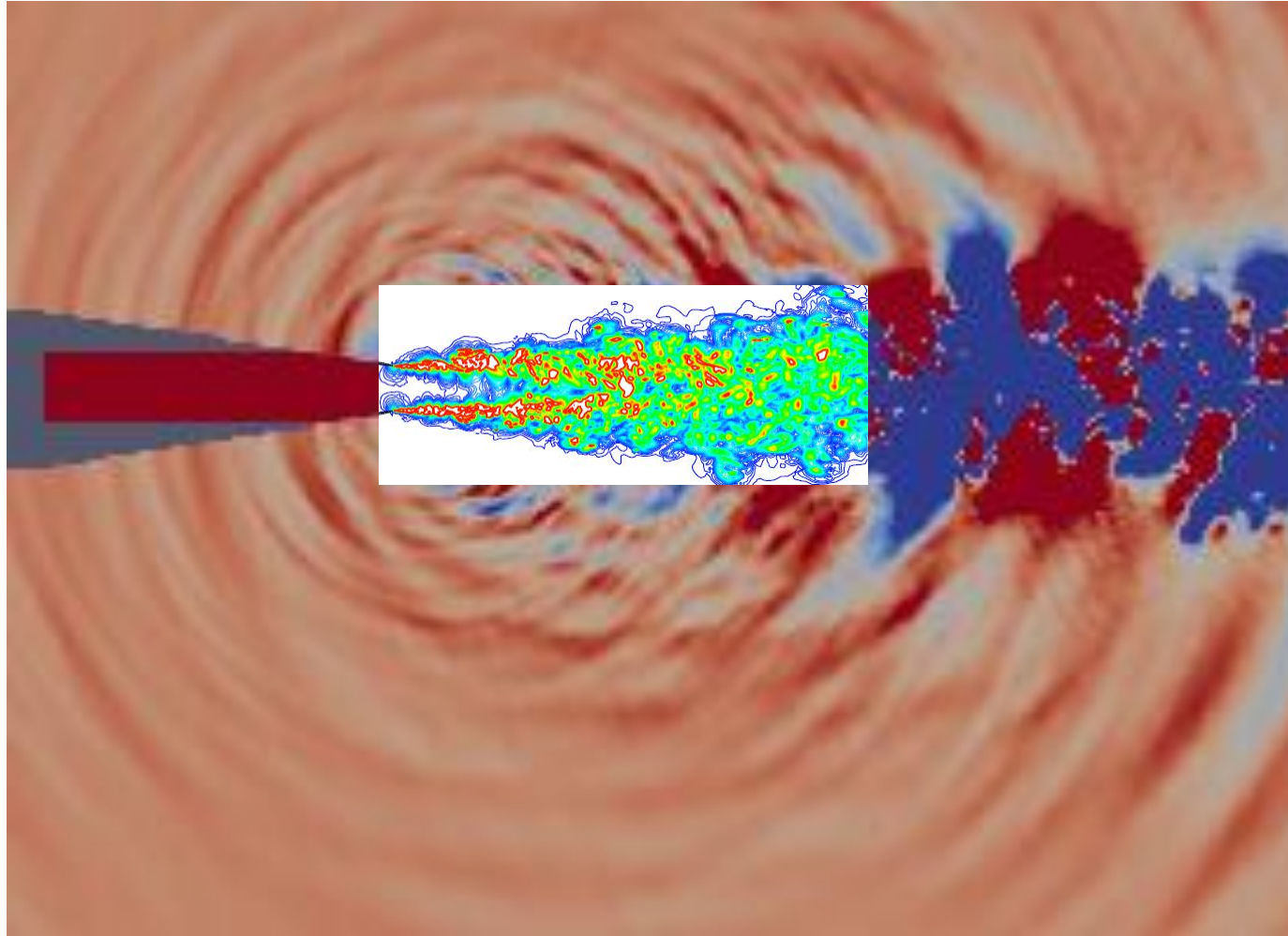


Comparison of two Goldstein acoustic analogy implementations with the Tam and Auriault model for heated and unheated jet noise prediction

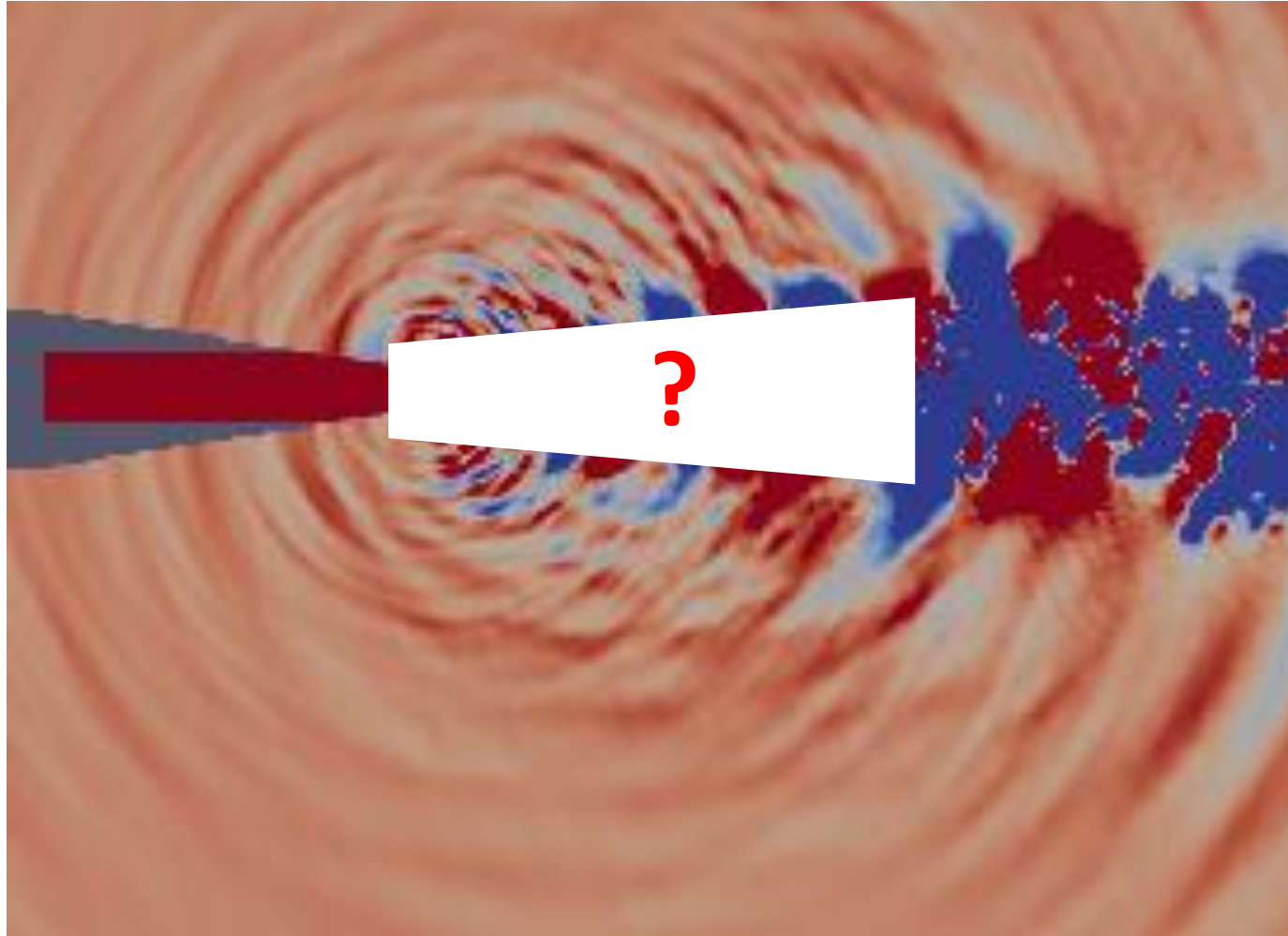
V. Gryazev, S. Karabasov

Queen Mary University of London

Jet Noise Problem



Mechanisms and sources



What does a jet noise source look like?



Blind monks examining an elephant, an ukiyo-e print by Hanabusa Itchō (1652–1724).

What does a jet noise source look like?



Examples of phenomenological a.k.a. “physical” approaches:
Two-source model (C.Tam)
Wavepackets (P.Jordan et al.)

What does a jet noise source look like?

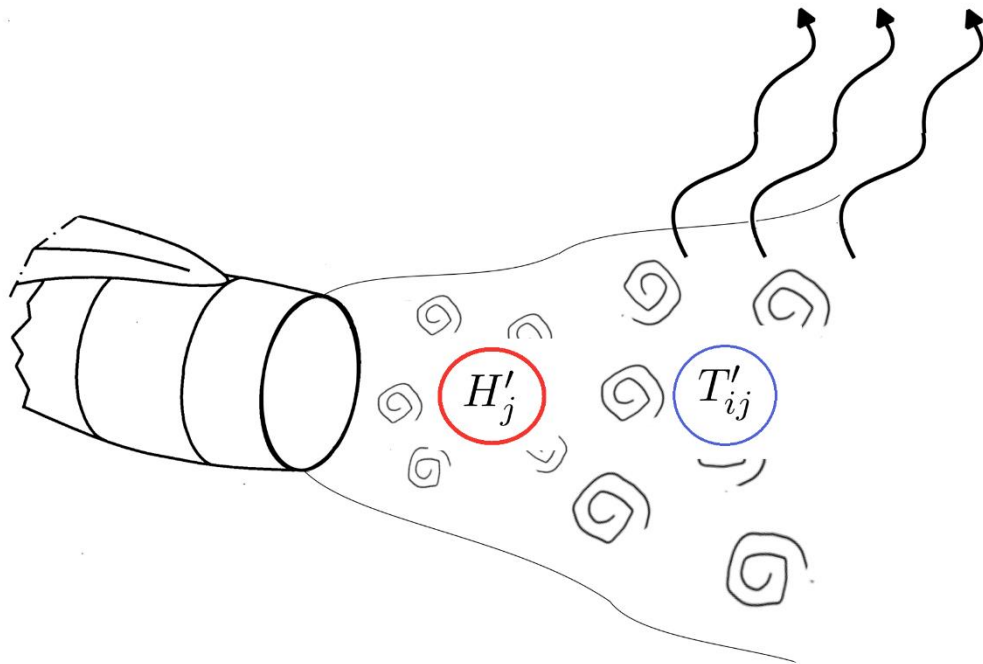


Examples of model decomposition a.k.a. “mathematical” approaches:
Acoustic analogy

Acoustic analogy models for heated jet noise prediction

Lighthill (1952), Lilley (1958), Ffowcs Williams (1963), Goldstein (2003)

Starts from NS eqs and systematically rearranges them to derive approximate models;
main assumption = sources don't depend on far-field noise propagation



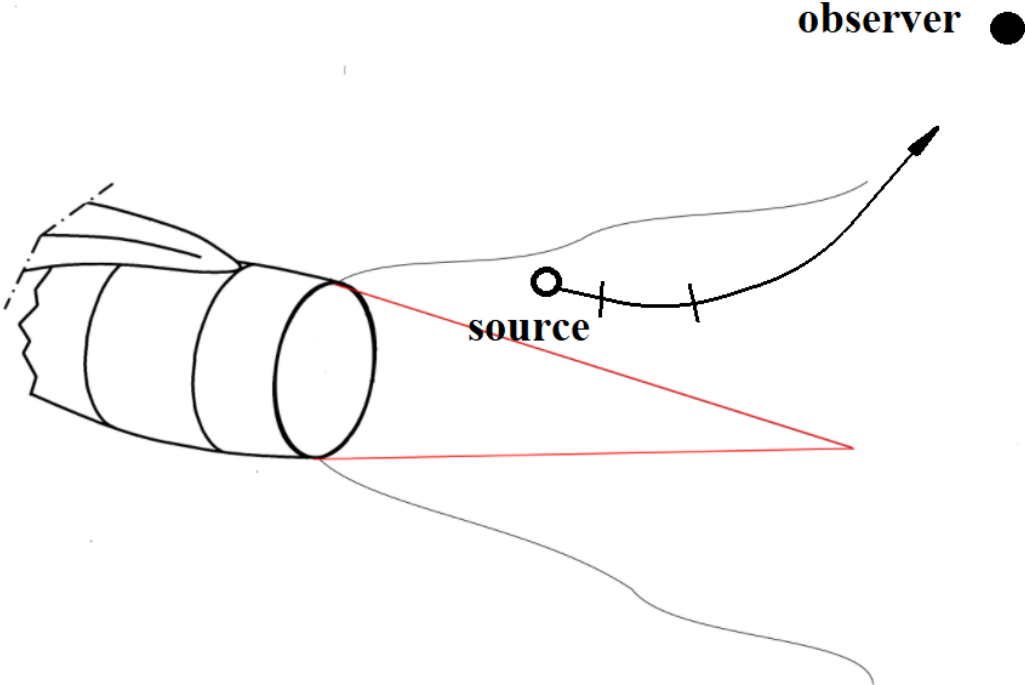
Fluctuating Reynolds stresses

T'_{ij}
cold jet
+

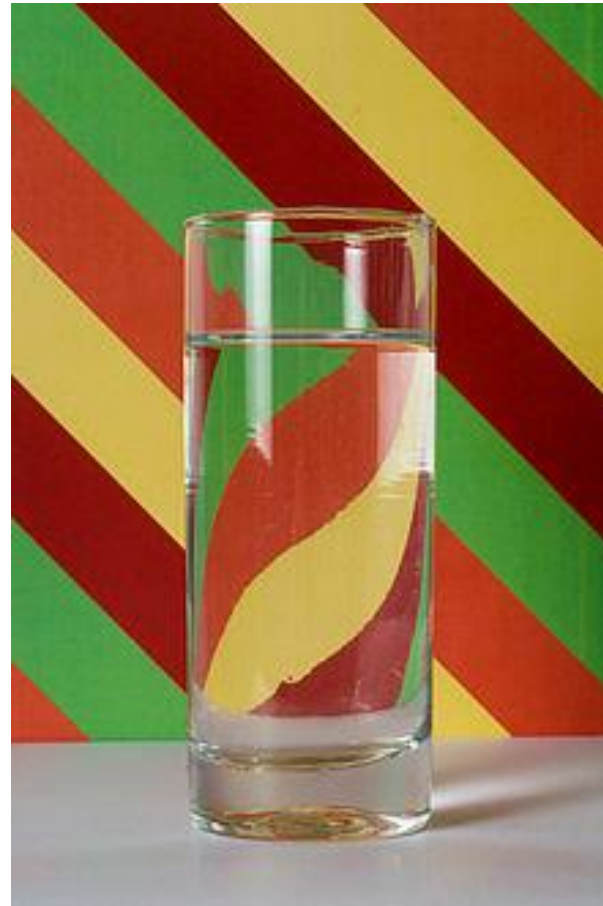
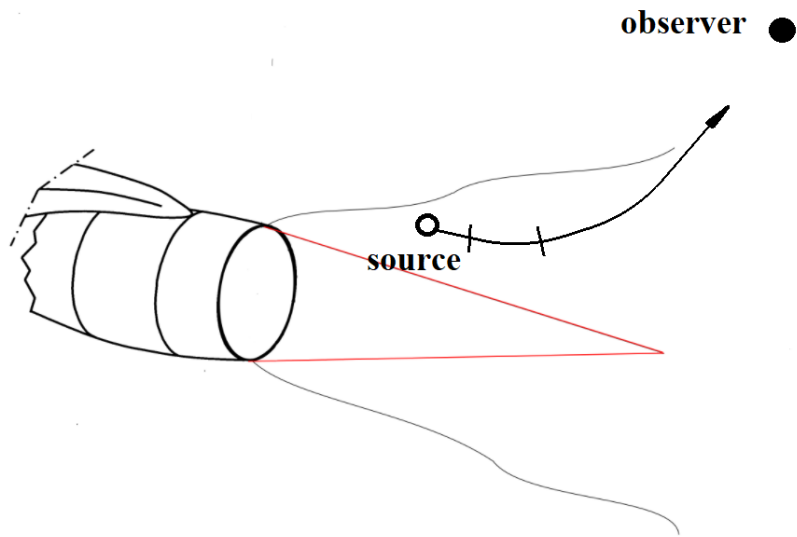
Enthalpy fluctuation source term

H'_j
hot jet

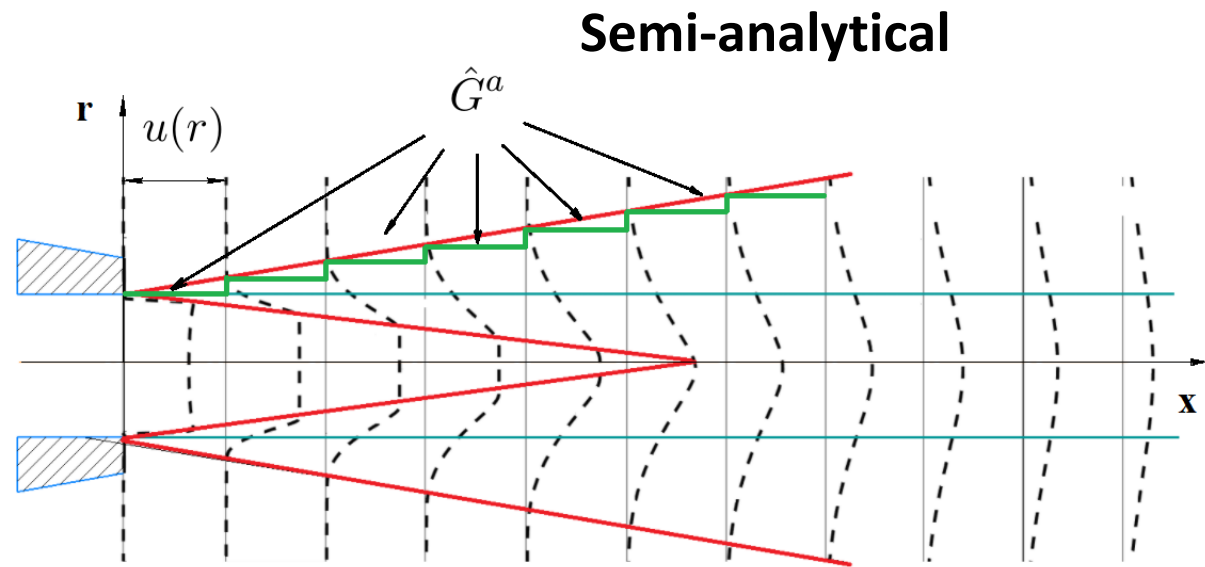
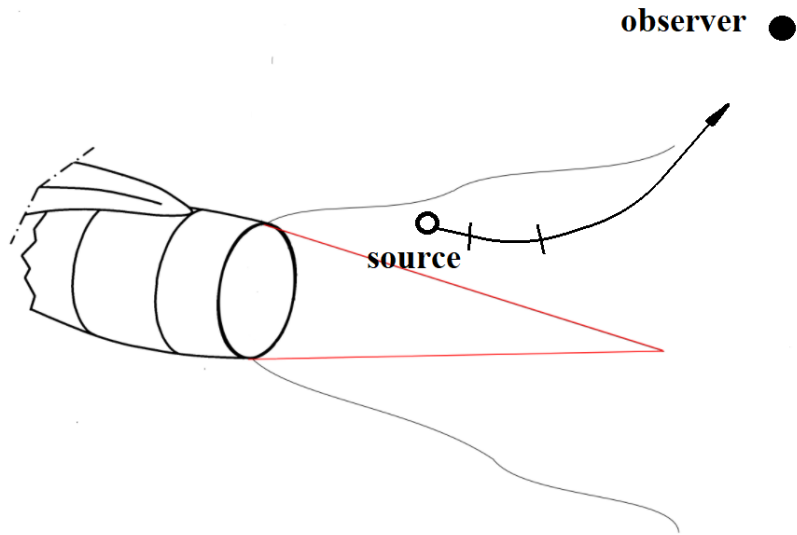
Meanflow refraction and thermal shear layer effects



Meanflow refraction and thermal shear layer effects



Sound propagation model: locally parallel flow approximation



Generalised Goldstein acoustic analogy

Starting from the exact rearrangement of NS equations, obtain expression for the far-field pressure in terms of the Green's function and the source terms:

$$\hat{p}(\mathbf{x}, \omega) = - \underbrace{\int_V \left(\hat{G}_i(\mathbf{y}, \omega; \mathbf{x}) \frac{\partial \hat{T}'_{ij}(\mathbf{y}, \omega)}{\partial y_j} \right)}_{\text{Cold}} + \underbrace{\hat{G}_4(\mathbf{y}, \omega; \mathbf{x}) \hat{Q}(\mathbf{y}, \omega)}_{\text{Cold + Hot}} dy,$$

where \hat{T}'_{ij} and \hat{Q} are the Fourier transform of the fluctuating Reynolds stresses and fluctuating enthalpy source

$$Q = \underbrace{-\tilde{v}_j \frac{\partial T'_{ij}}{\partial y_i} + \frac{\delta_{ij}}{2} \left[\frac{DT'_{ij}}{D\tau} + \frac{\partial \tilde{v}_k}{\partial y_k} T'_{ij} \right]}_{\text{Cold}} - \underbrace{\frac{\partial}{\partial y_j} (\rho v''_j h''_0 - \bar{\rho} v''_j h''_0)}_{\text{Hot}}$$

Model 1: Khavaran and Bridges (2010)

$$\overline{p^2}(\mathbf{x}, \mathbf{y}, \omega) = \left[\begin{array}{l} A \cdot [I_{1111} f(\theta, M, \kappa)] + \\ B \cdot [I_{1111} f(\theta, M, \kappa, c, h', \tilde{h})] \end{array} \right] \cdot \frac{\sum_{n=0}^{\infty} (1 + \delta_{n0}) f_n f_n^*}{(1 - M_c \cos \theta)^2}$$

← cold
← hot

Ignore the source directivity + put the sources in the moving frame of the jet

Empirical calibration constants: c_l, c_τ and A, B + the convection speed calibration

Model 2: Tam and Auriault (1999)

$$p(\mathbf{x}, t) = \int_V \int_{-\infty}^{\infty} \left(\int_{-\infty}^{\infty} p_a(\mathbf{x}, \mathbf{x}_1, \omega) \exp(-i\omega(t - t_1)) d\omega \right) \times \frac{Dq_s(\mathbf{x}_1, t_1)}{Dt_1} dt_1 d\mathbf{x}_1$$

The source is modelled statistically in accordance with the Gaussian representation of the appropriate two-time two-space auto-correlation function

$$\overline{\frac{Dq_s(\mathbf{x}_1, t_1)}{Dt_1} \frac{Dq_s(\mathbf{x}_2, t_2)}{Dt_2}} \sim \frac{\hat{q}_s^2}{c^2 \tau_s} \exp\left[-\frac{|\xi|}{\bar{u} \tau_s} - \frac{\ln 2}{l_s^2} \left((\xi - \bar{u} \tau)^2 + \eta^2 + \zeta^2 \right)\right]$$

Ignore the source directivity and cold/hot source type differences + put the sources in the moving frame of the jet

Empirical calibration constants c_l, c_τ and A

Model 3 (Karabasov et al. 2010 + hot sources)

The idea

$$R'_{\text{Hot},ij}(\mathbf{y}, \tau) \approx \overline{\rho^2} \overline{(h''_0)^2} \overline{v''_i(\mathbf{y}, t) v''_j(\mathbf{y} + \Delta, t + \tau)}$$

Keep the source directivity + keep the sources in the nozzle (lab) frame

$$\hat{P}(\mathbf{x}, \omega) = \int_V \left(\overbrace{A_{ijkl}(\mathbf{y}) W(\mathbf{y}) \hat{I}_{ij} \hat{I}_{kl}^*}^{\hat{F}_{\text{Cold}}} + \overbrace{B_{ij}(\mathbf{y}) W(\mathbf{y}) \frac{\partial \hat{G}_4^a}{\partial y_i} \frac{\partial \hat{G}_4^{a*}}{\partial y_j}}^{\hat{F}_{\text{Hot}}} \right) d\mathbf{y}$$

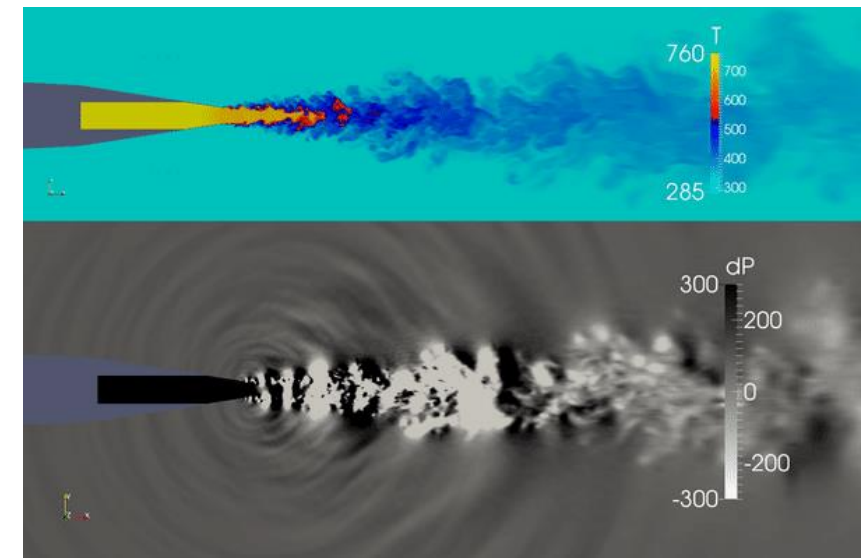
$$A_{ijkl}(\mathbf{y}) = \underbrace{C_{ijkl}^A}_{\text{quadrupole}} (2\bar{\rho}\bar{\kappa})^2, \quad B_{ij}(\mathbf{y}) = \underbrace{C_{ij}^B}_{\text{dipole}} \rho_\infty c_\infty^4 \bar{\rho}\bar{\kappa} \frac{\overline{h_t'^2}}{h^2}$$

Use the Khavaran and Bridges empirical scaling law

Empirical calibration constants: c_l, c_τ and A, B

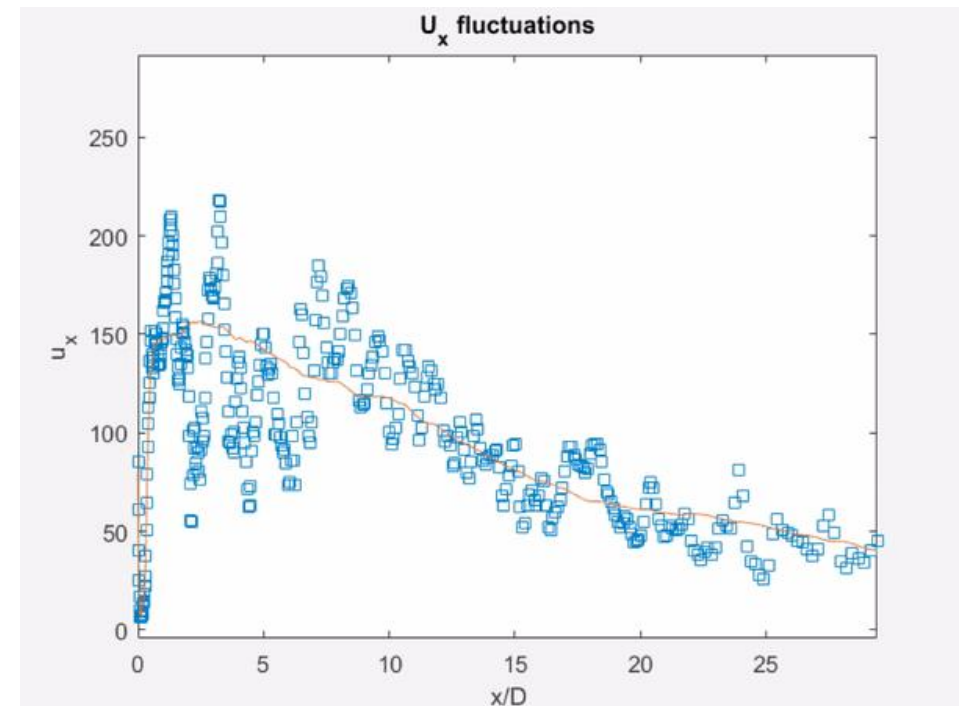
+ coeff. R_{ijkl}/R_{1111} and R_{ij}/R_{11}
(can be derived from LES)

SILOET LES: CABARET



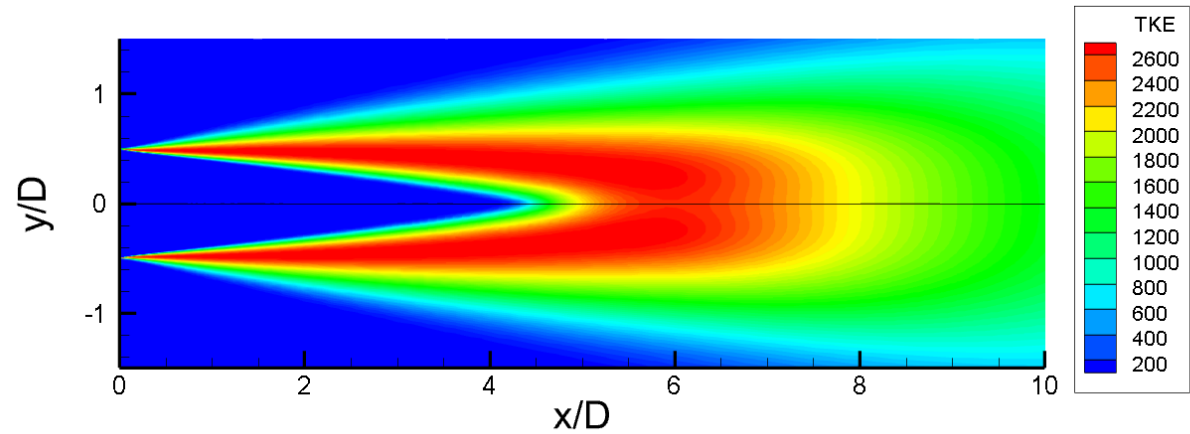
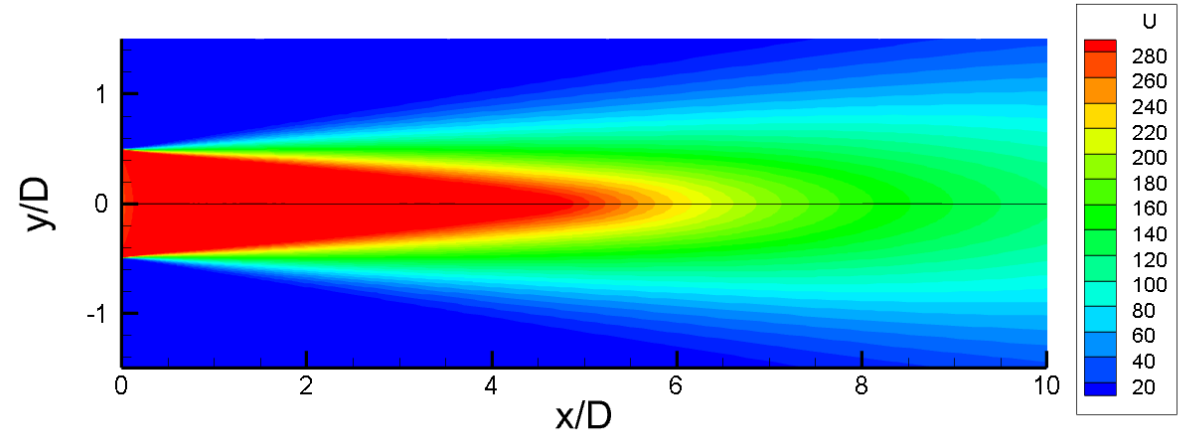
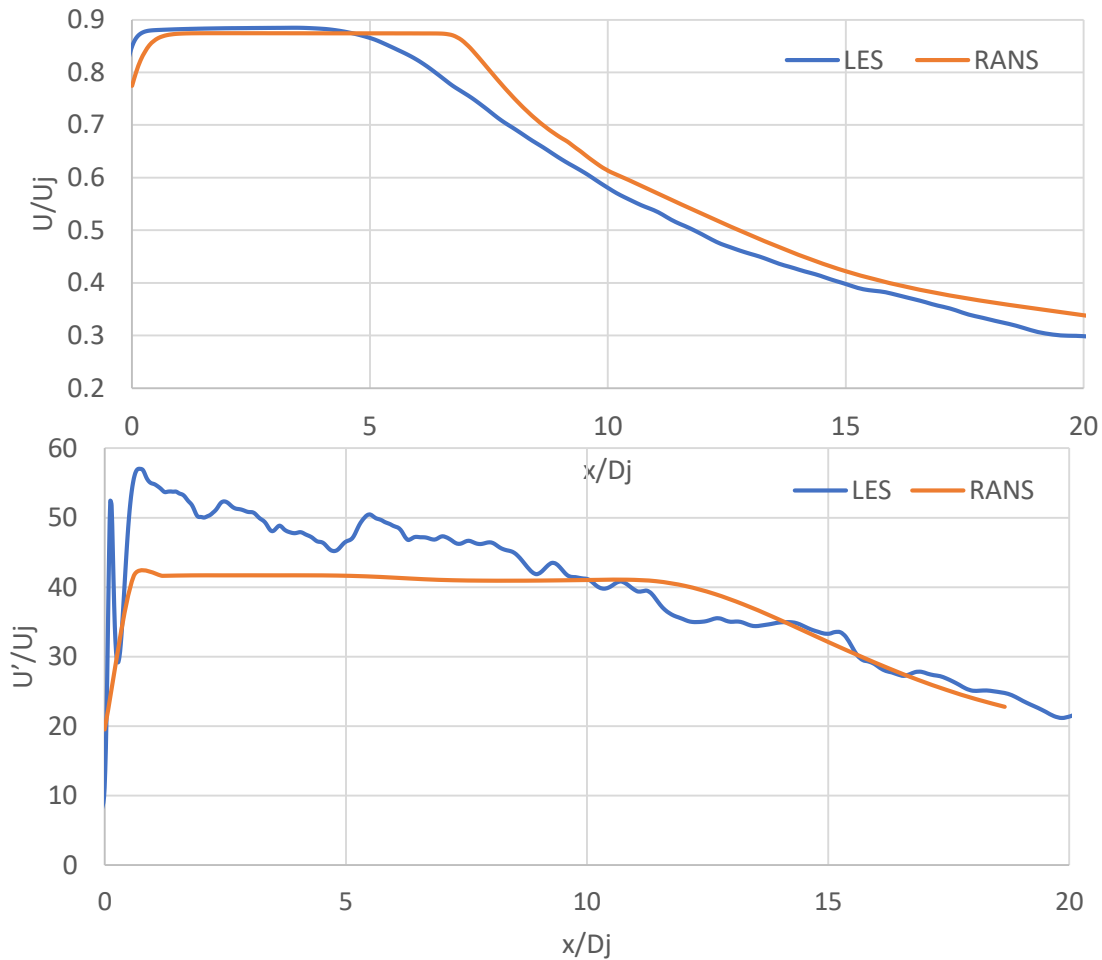
Jet cases:

- **static isothermal SILOET jet**
 $V_j/c_0=0.875$ $T_j/T_0=1$
- **static heated SILOET jet**
 $V_j/c_0=0.875$ $T_j/T_0=2.5$
 $ReD \sim 2-4 \cdot 10^6$



Use the LES solution to obtain velocity fluctuations in a small part of the jet (lipline)

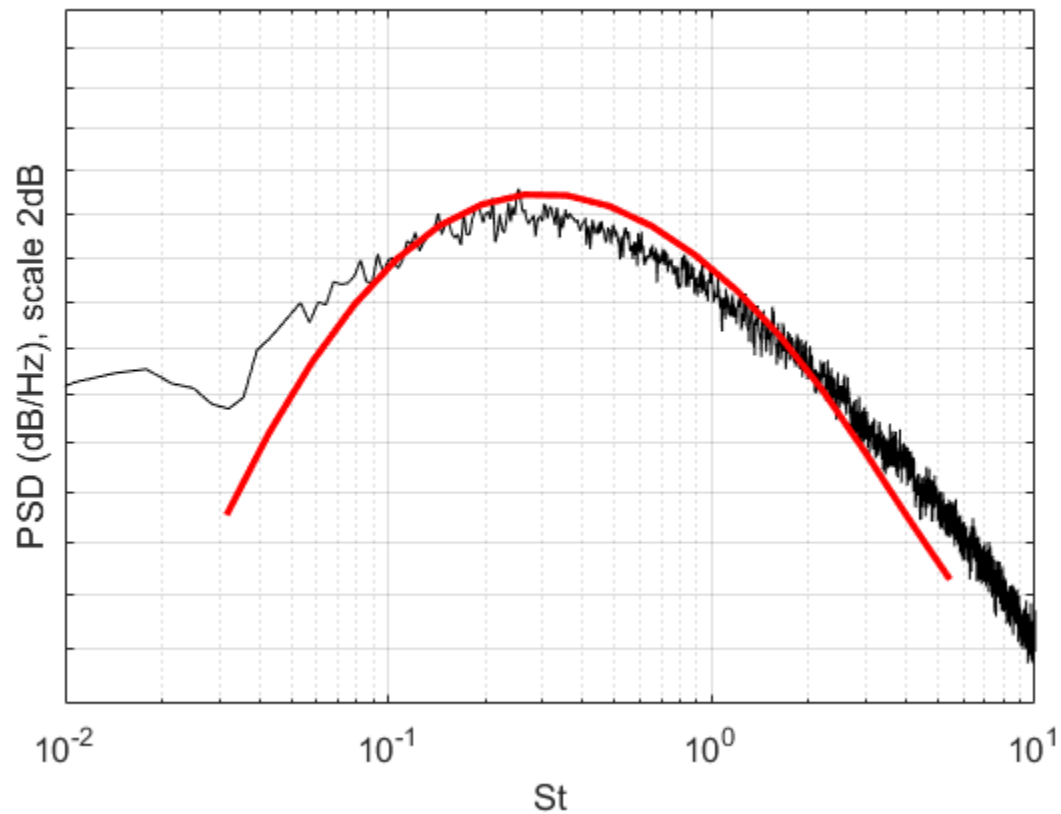
SILOET RANS: ANSYS Fluent



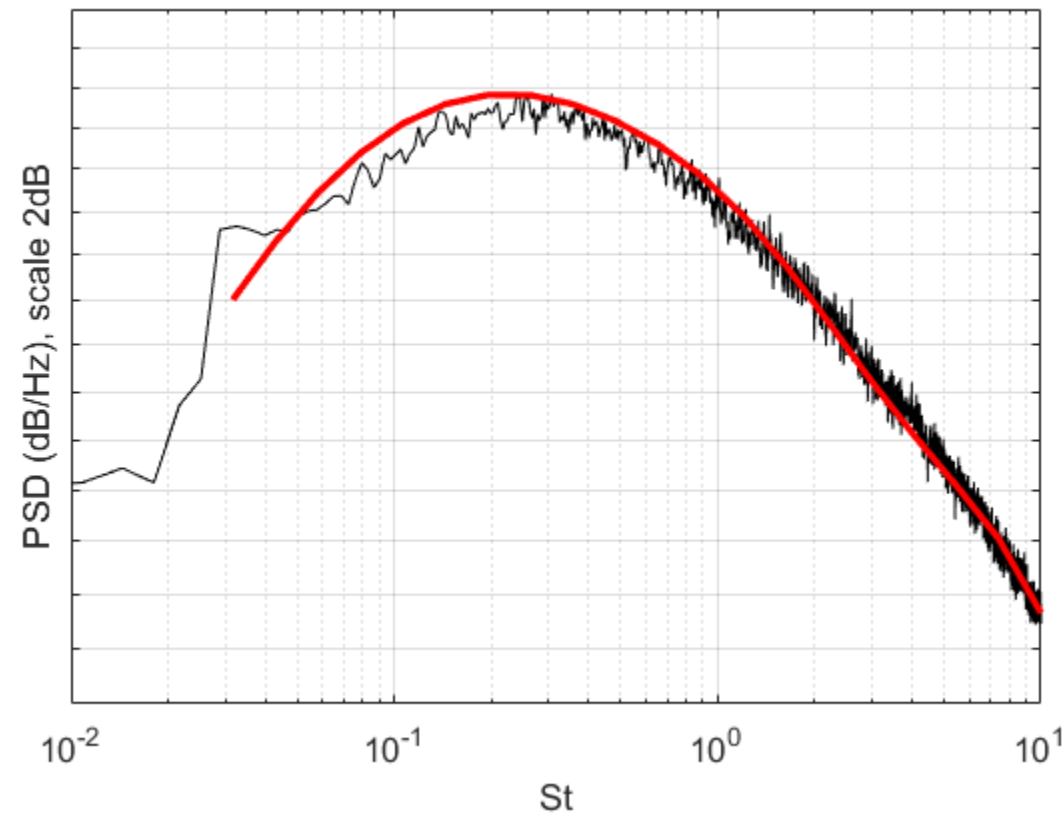
=> low-order models of the jet noise sources implemented in Matlab

Model 1 (Khavaran and Bridges)

cold



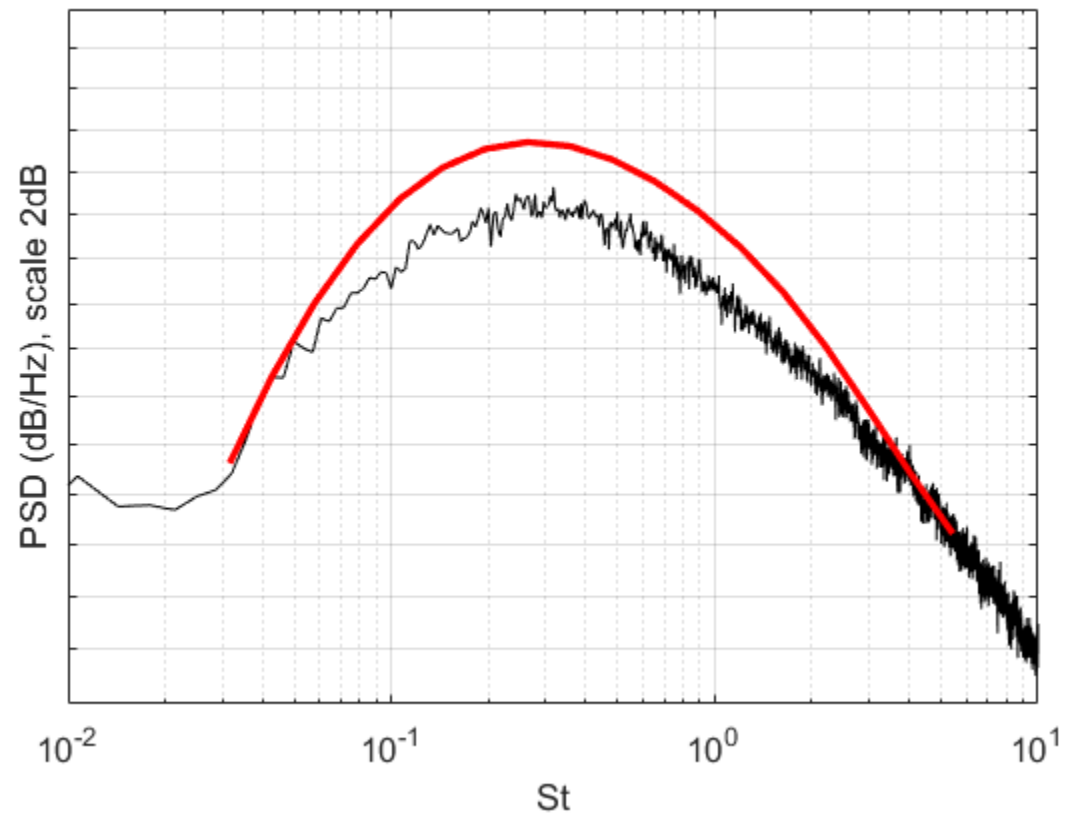
hot



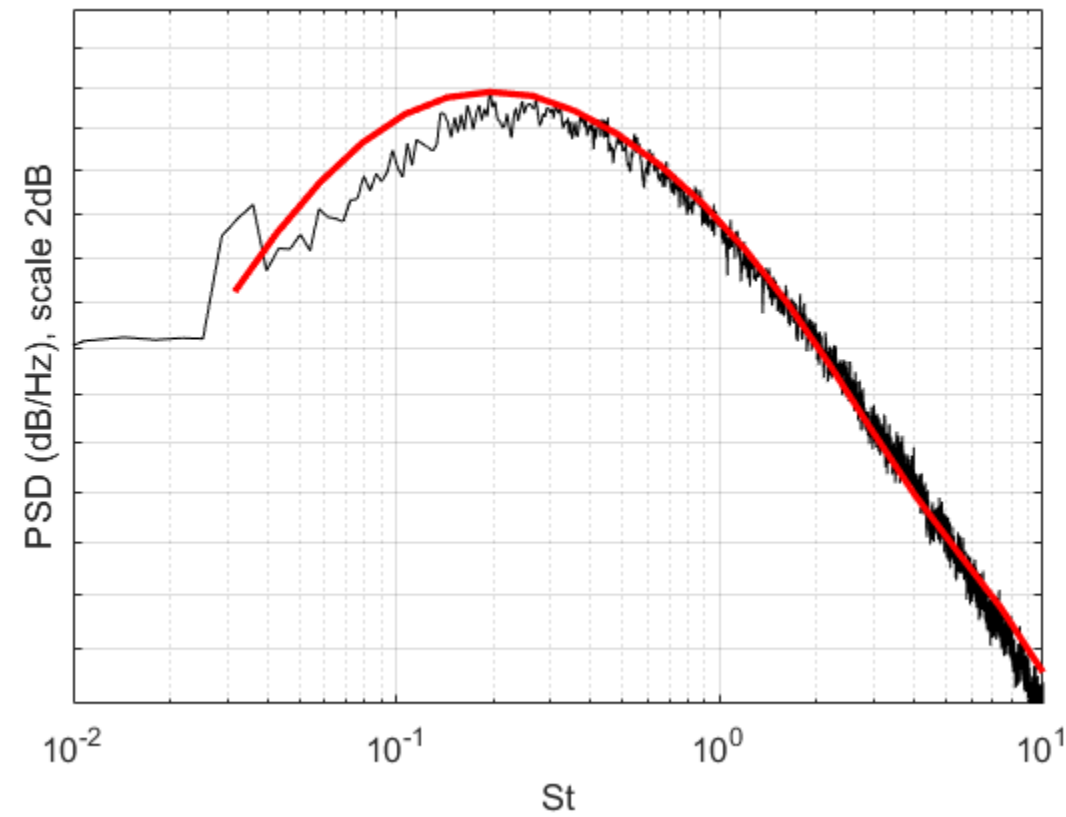
Observer angle = 90°

Model 1

cold



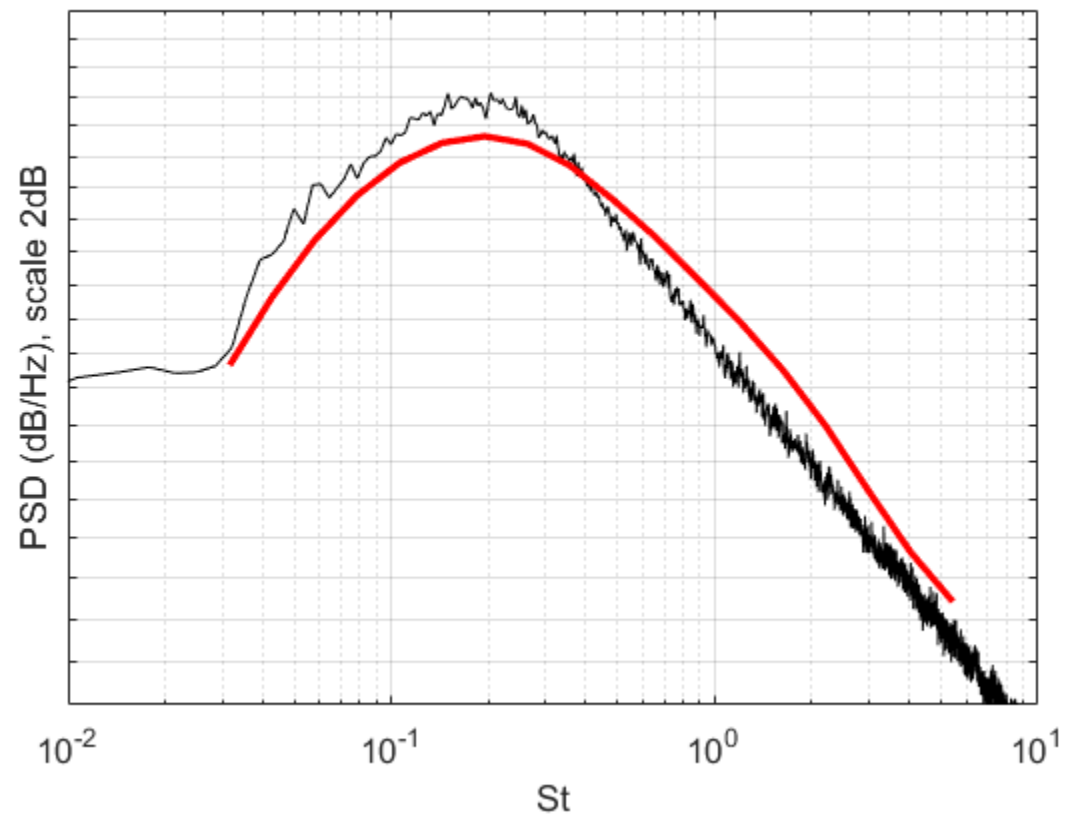
hot



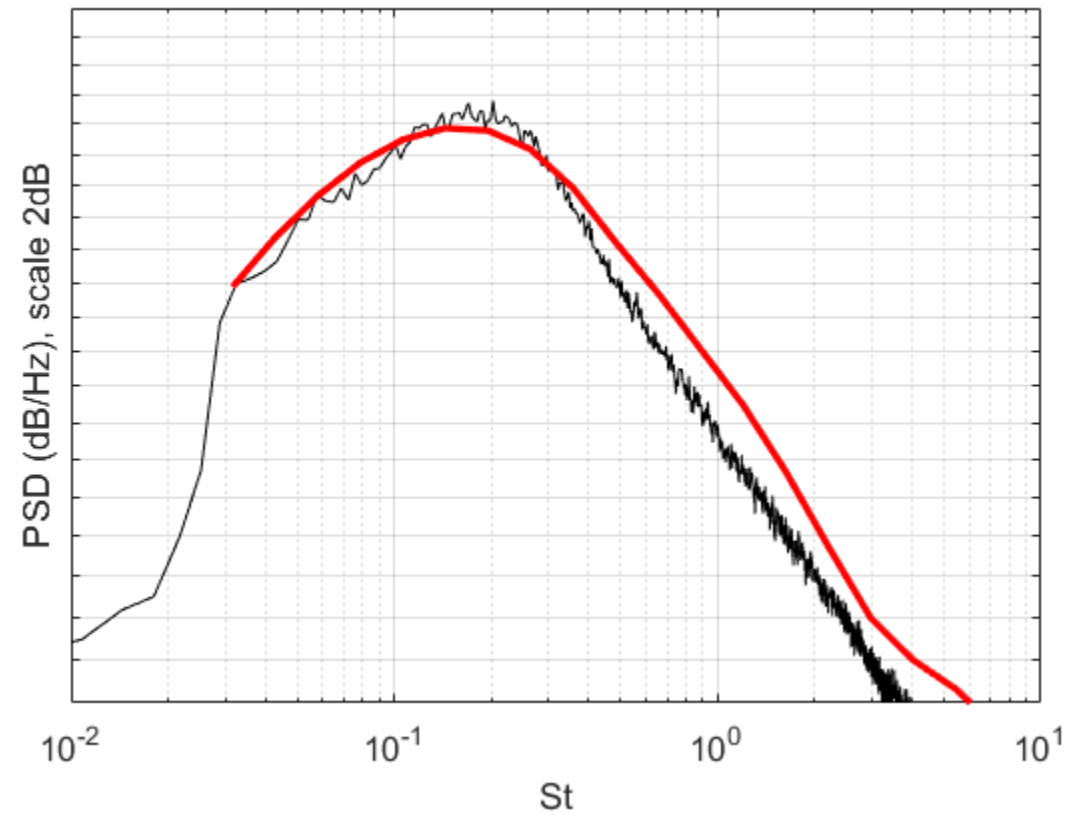
Observer angle = 60°

Model 1

cold



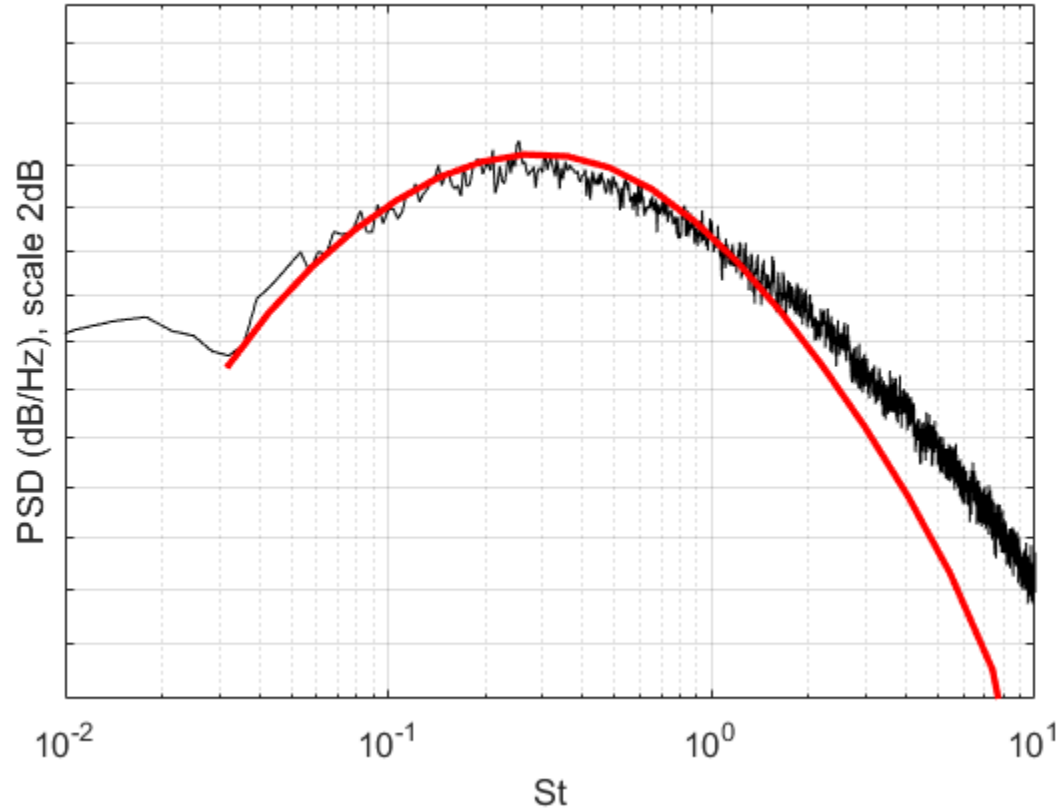
hot



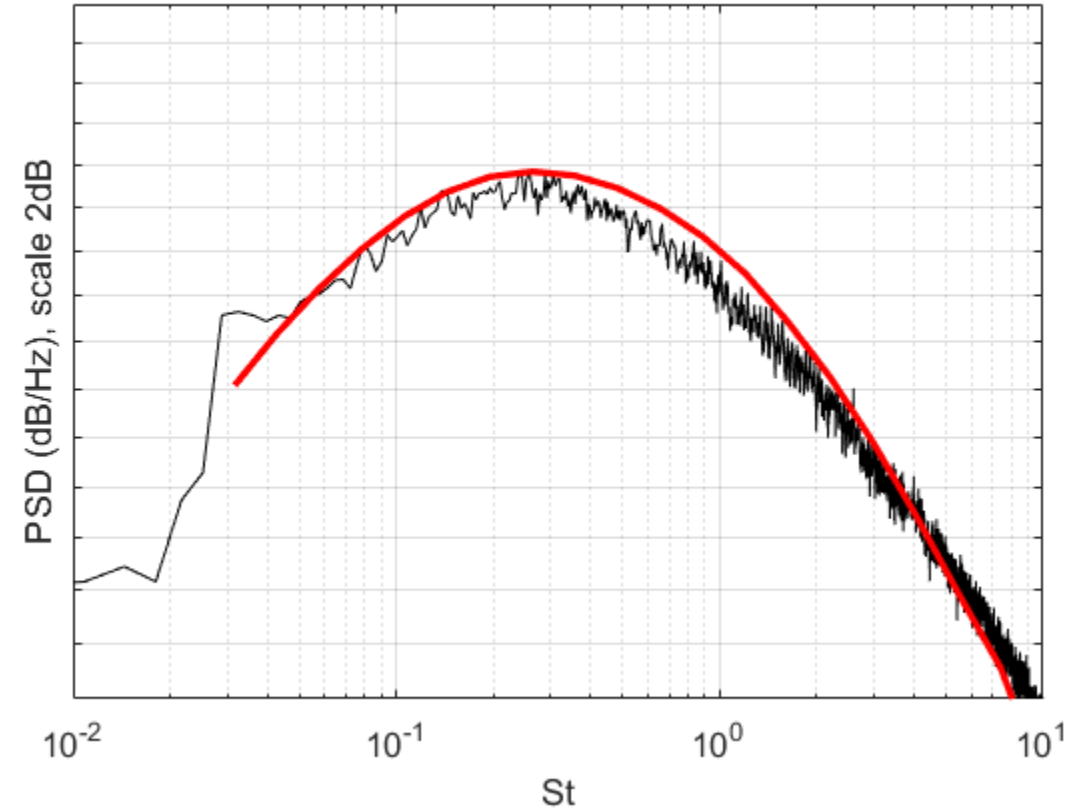
Observer angle = 30°

Model 2 (Tam and Auriault)

cold



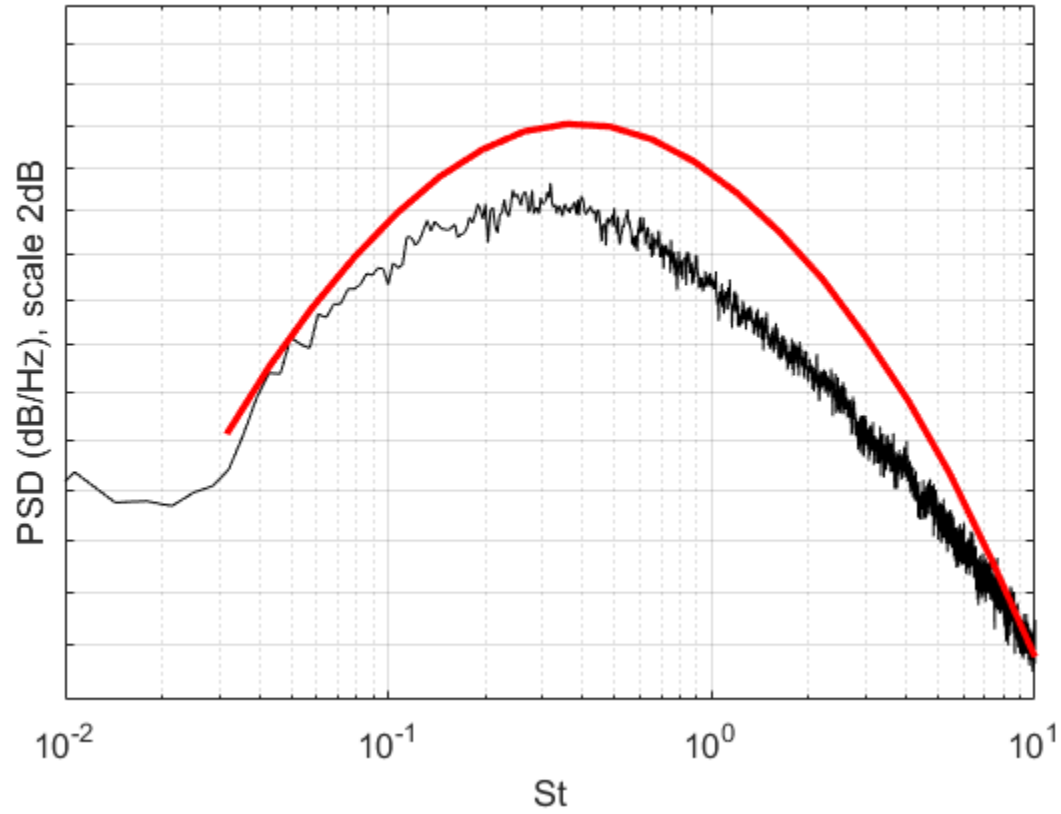
hot



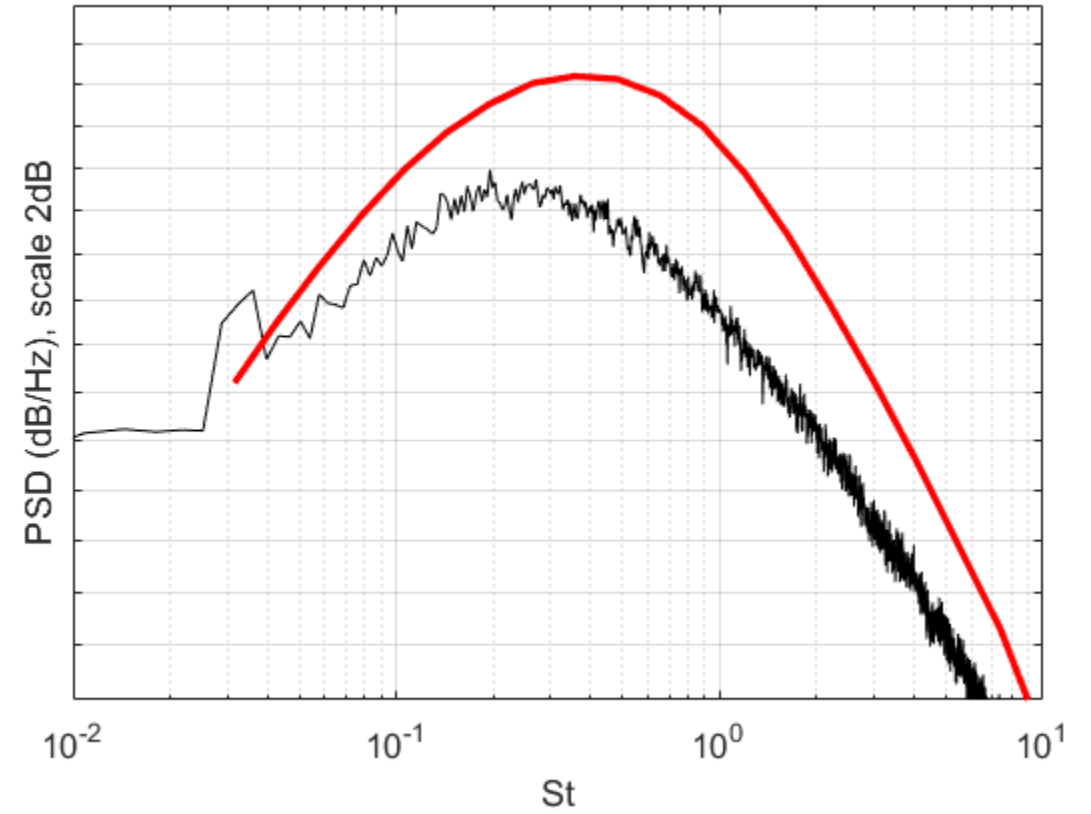
Observer angle = 90°

Model 2

cold



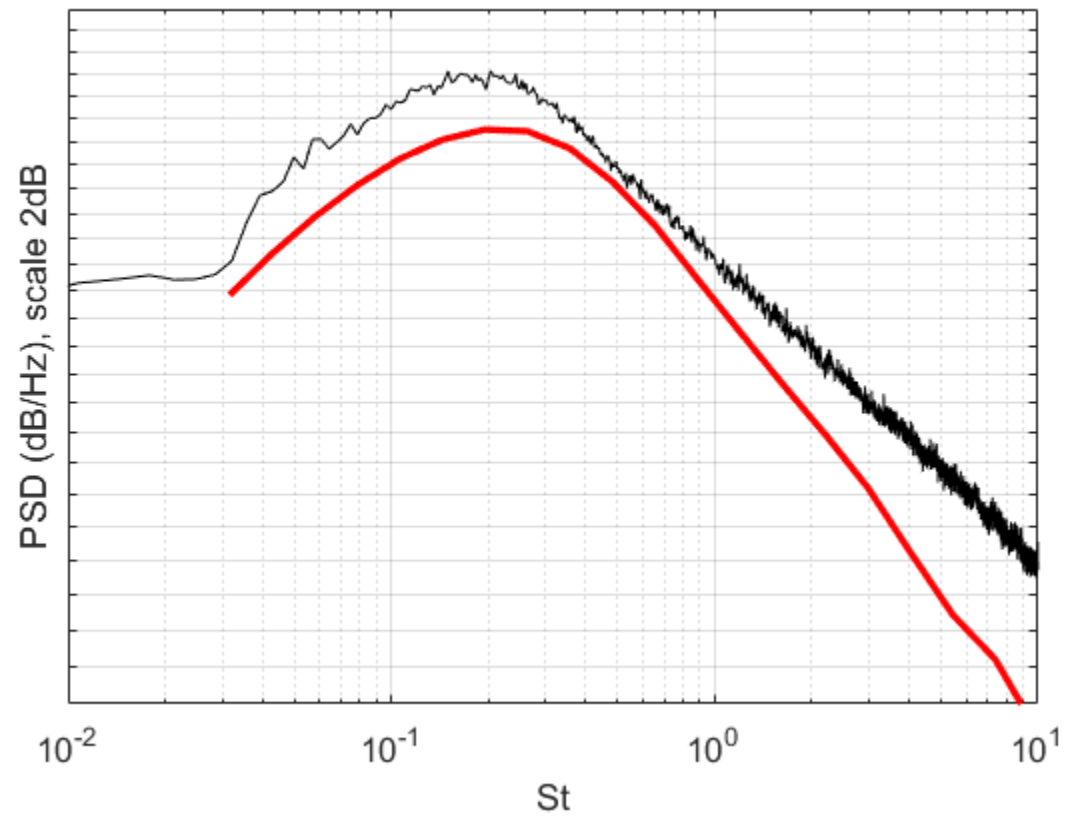
hot



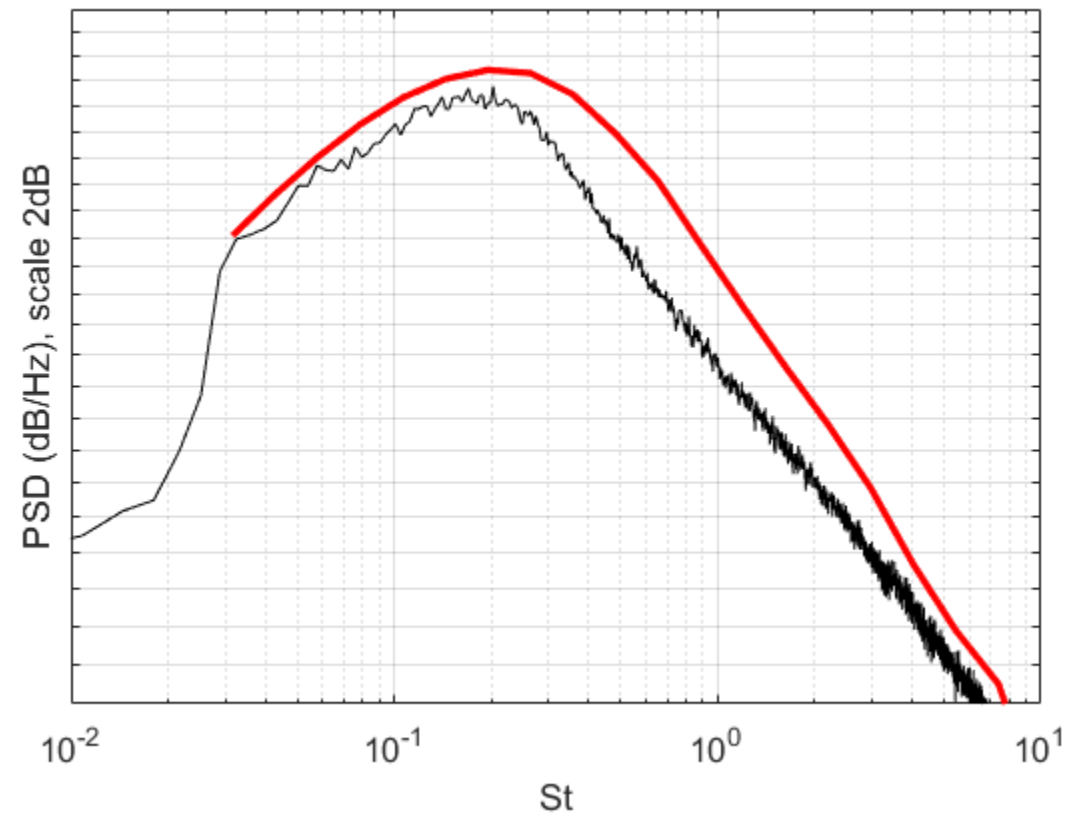
Observer angle = 60°

Model 2

cold



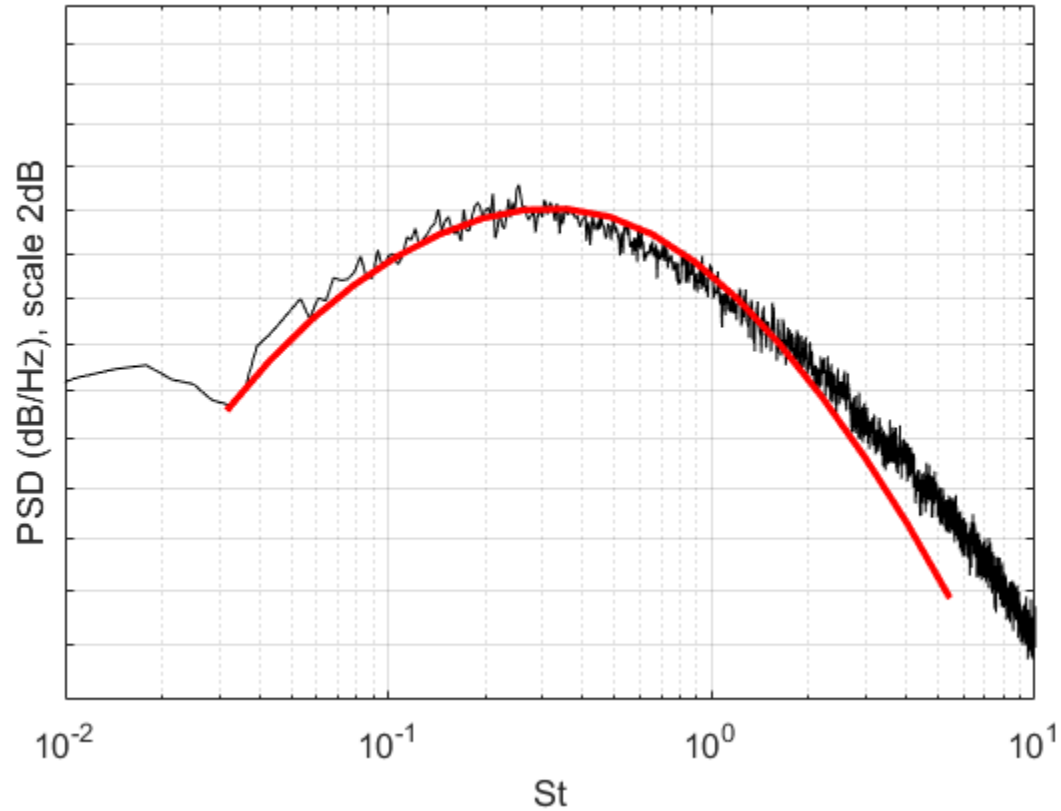
hot



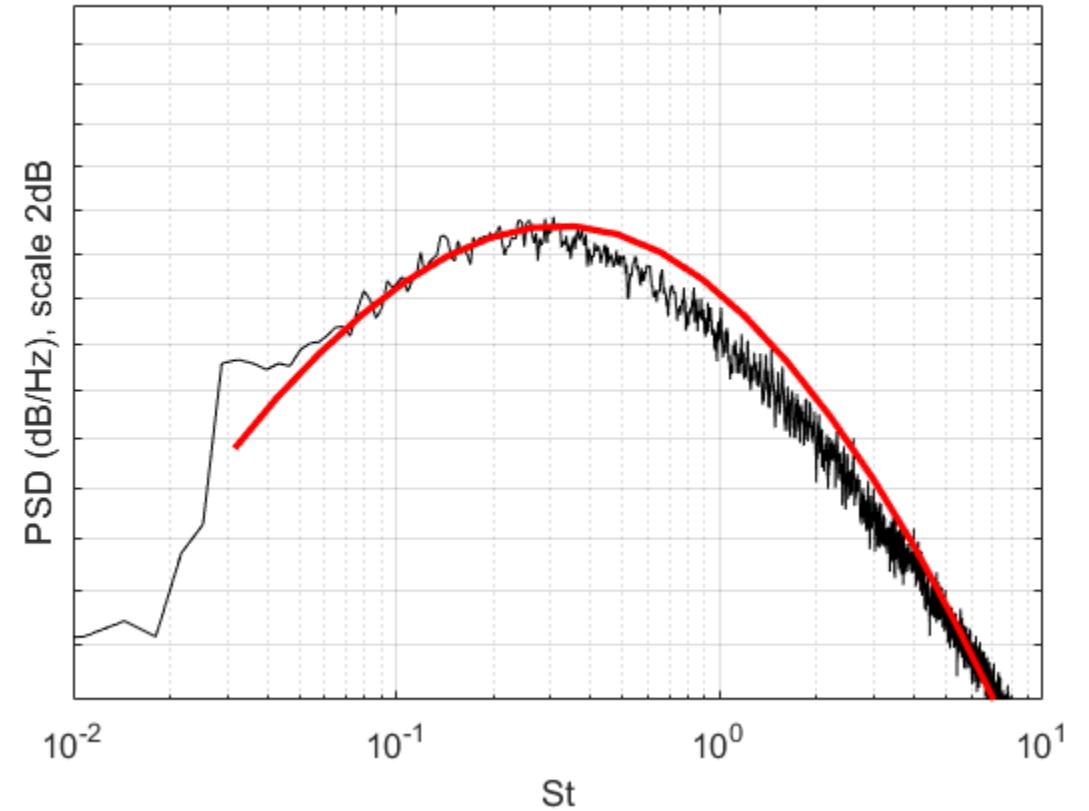
Observer angle = 30°

Model 3 (New=Karabasov et al. 2010 + hot sources)

cold



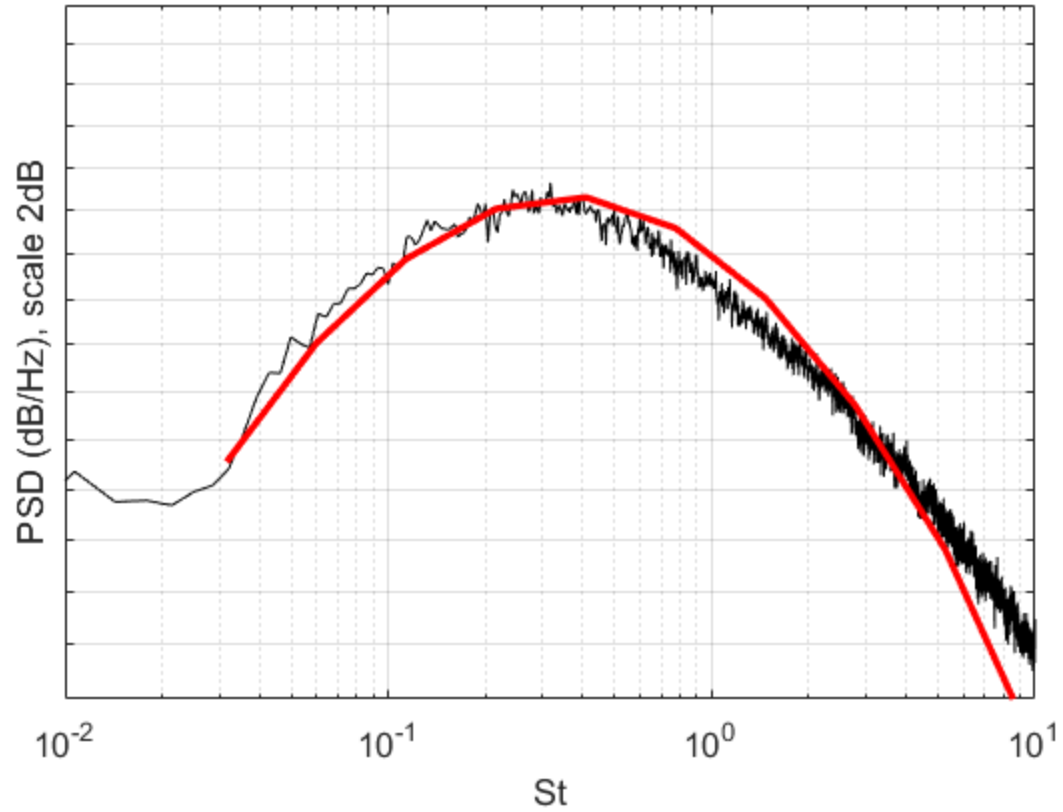
hot



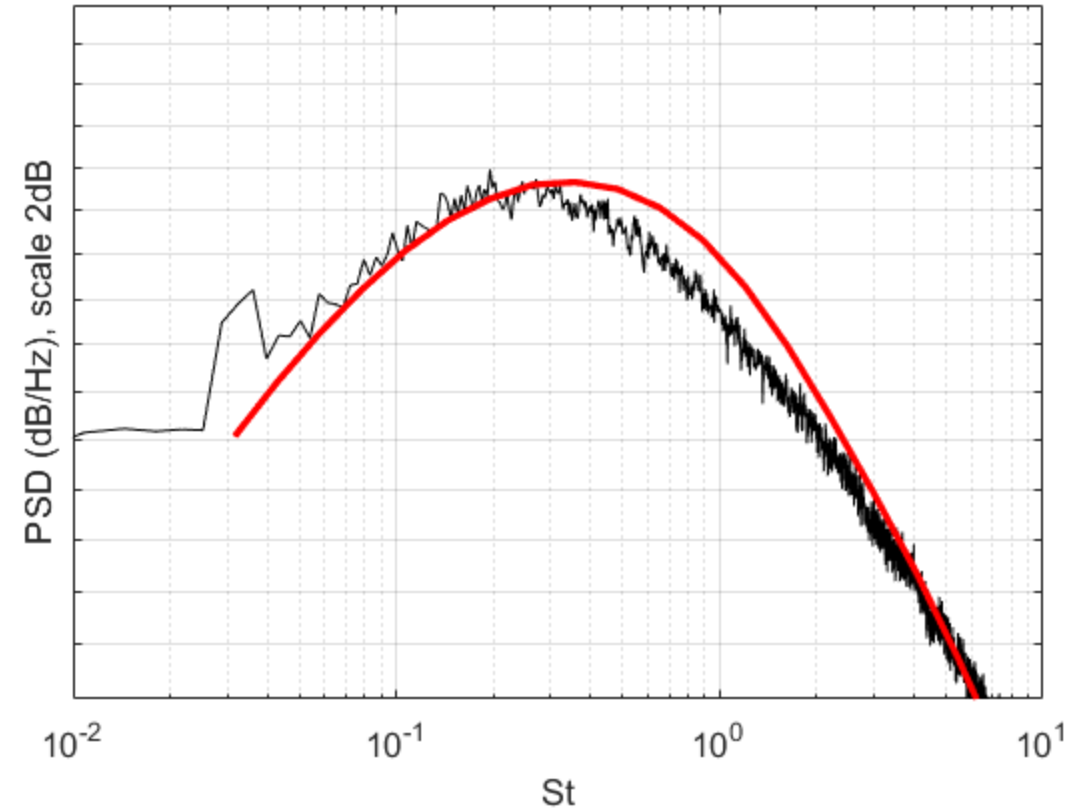
Observer angle = 90°

Model 3

cold



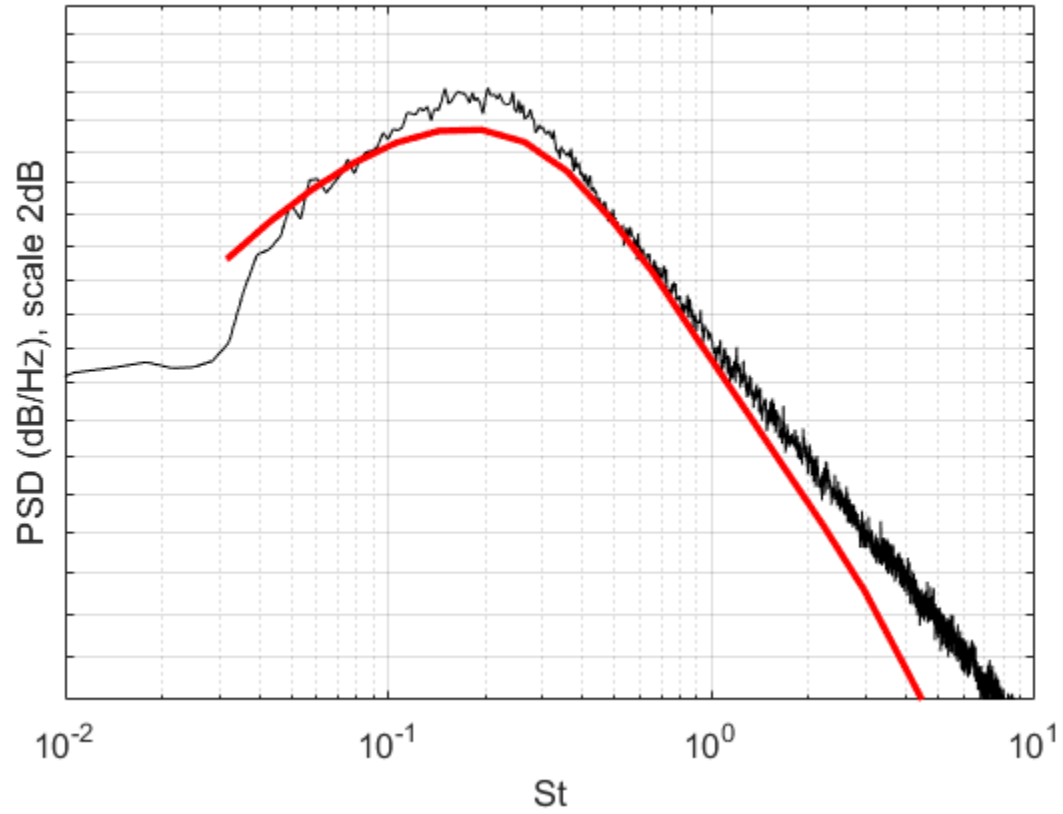
hot



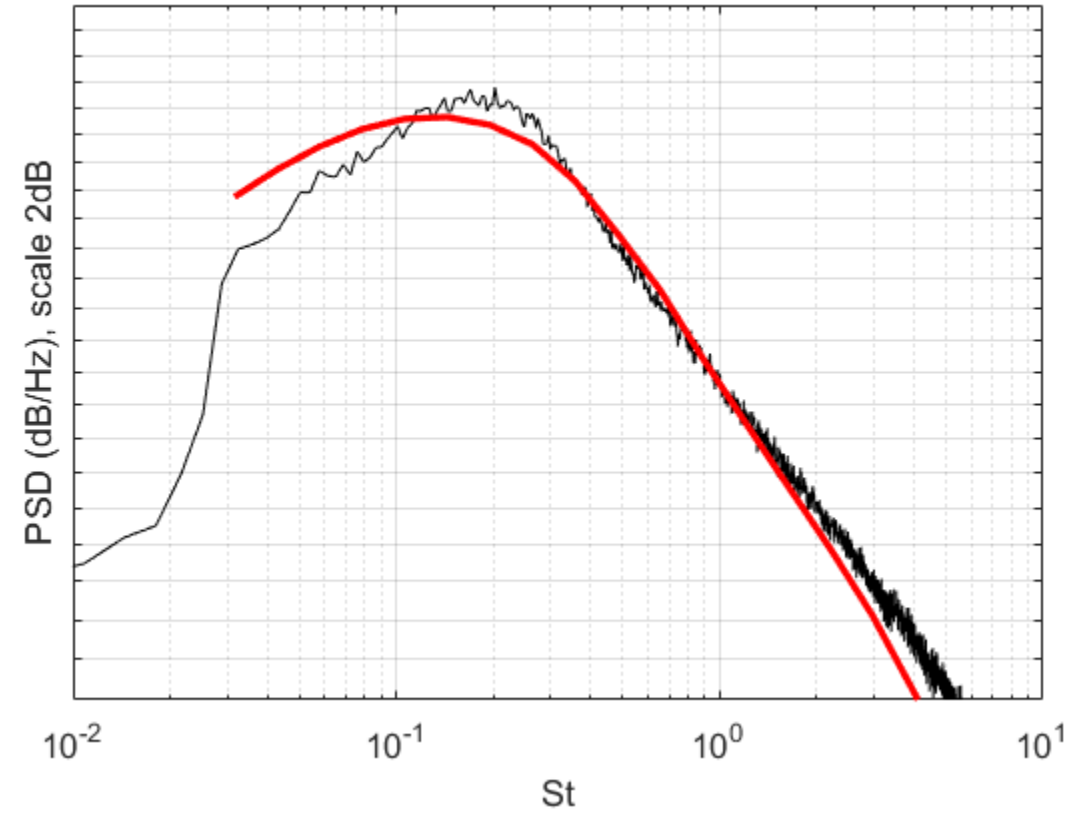
Observer angle = 60°

Model 3

cold



hot

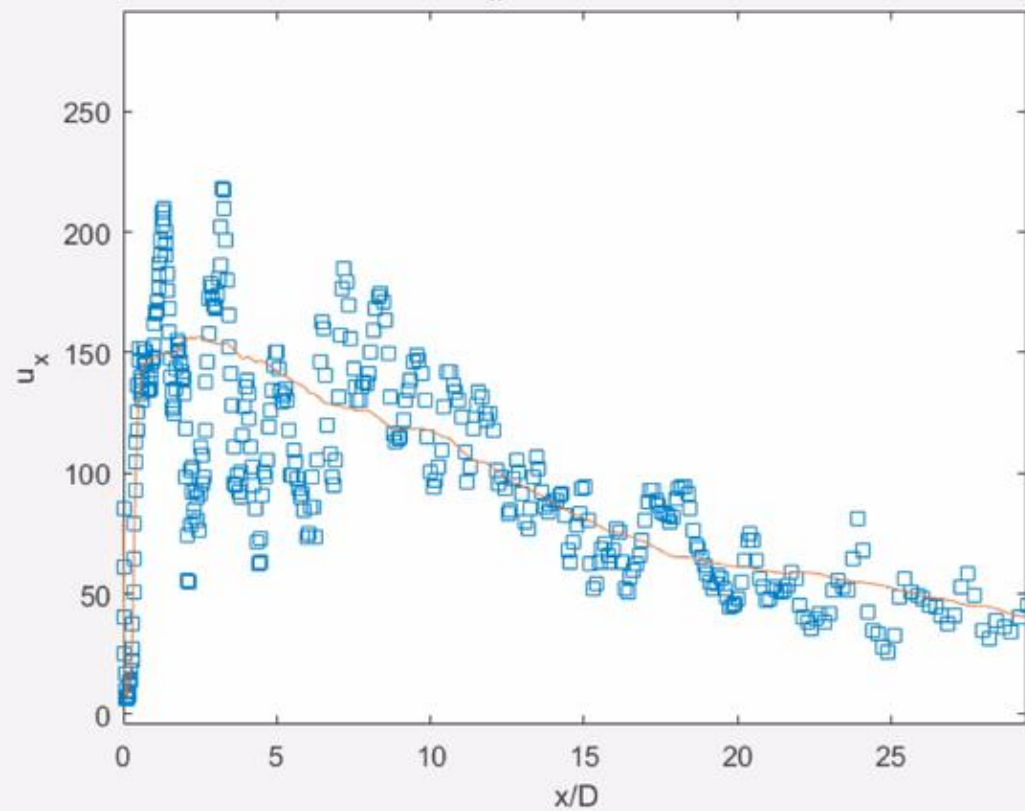


Observer angle = 30°

Conclusion

- A new model based on a combination of the Goldstein acoustic analogy implementation from Karabasov et al. (2010) and the Khavaran and Bridges model (2010) has been developed
- The model has been validated for the heated and unheated SILOET jet experiment and a 2-3dB accuracy is reported for a good range of polar angles and frequencies corresponding to $0.04 < St < 2-3$. It outperforms the standard low-order jet noise models.

U_x fluctuations



Non-dimensional source amplitudes

ij,kl	11,11	22,22	33,33	12,12; 12,21; 21,12; 21,21	13,13; 13,31; 31,13; 31,31;	23,23; 23,32; 32,23; 32,32;
	0.64	0.114	0.17	0.175	0.175	0.069

Table 1. Quadrupole source

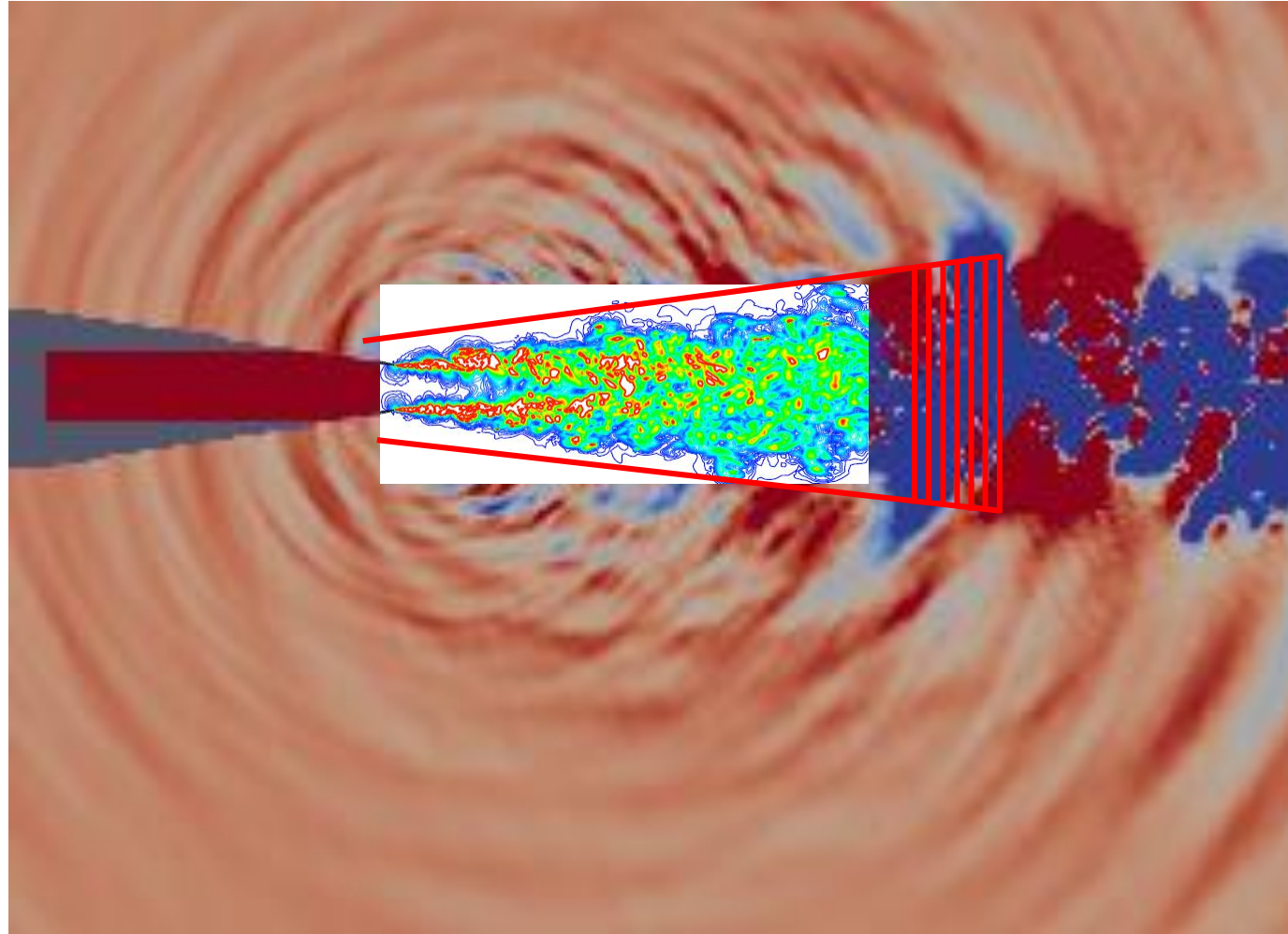
i,j	11,11	22,22	33,33	12,12	13,13	23,23
	1.06	0.47	0.47	0.7	0.7	0.479

Table 3. Dipole source

ij,kl	11,11	22,22	33,33	12,12; 12,21; 21,12; 21,21	13,13; 13,31; 31,13; 31,31;	23,23; 23,32; 32,23; 32,32;
	1	0.33	0.3	0.37	0.37	0.15

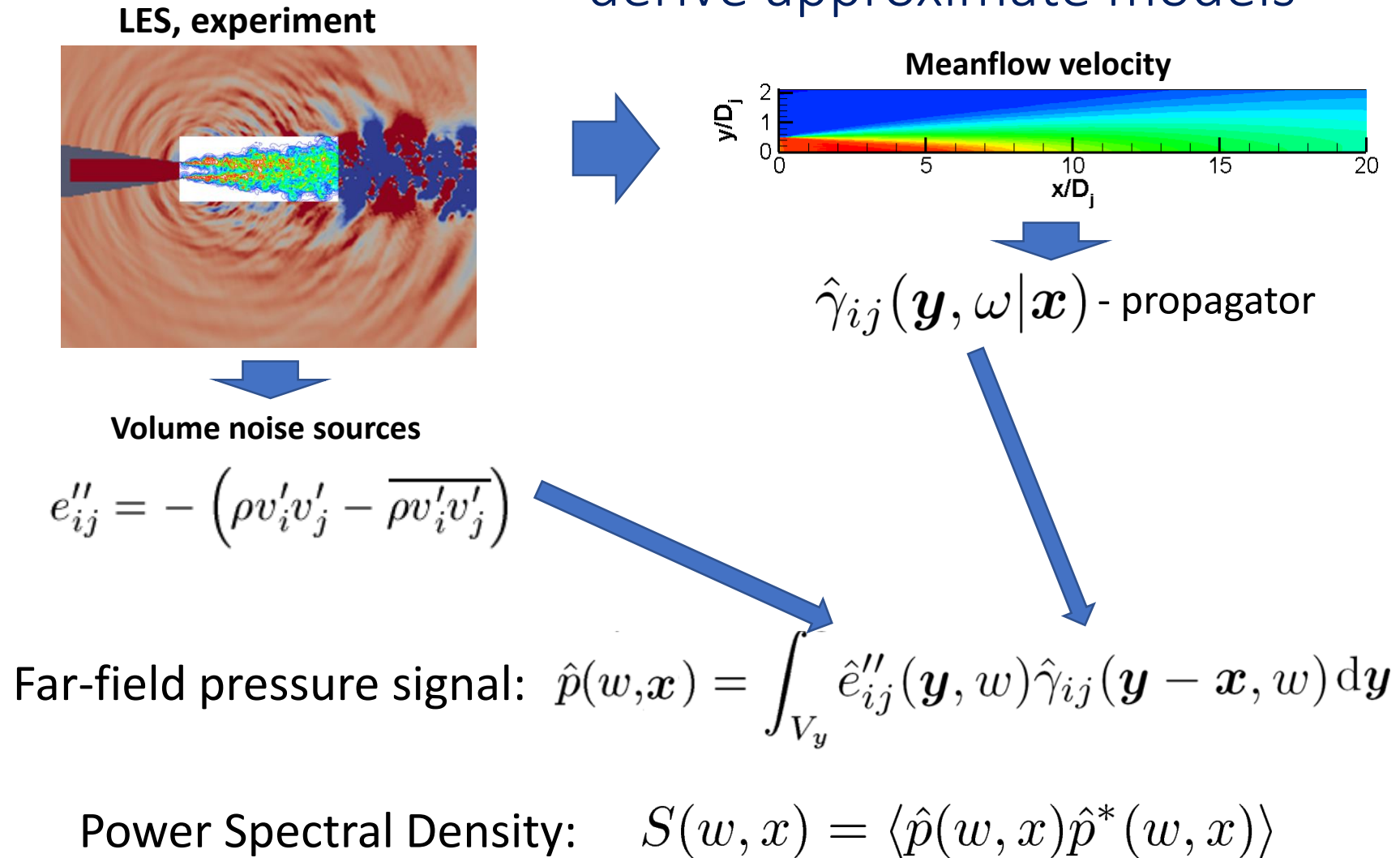
Table 3. Quadrupole source (Karabasov 2010)

Computational domain decomposition: integral methods



Lighthill (1952), Lilley (1958), Ffowcs Williams (1963), Goldstein (2003)

Acoustic analogy: starts from NS and systematically rearranges them to derive approximate models



Model 1: Khavaran and Bridges (2010)

The far-field spectral density is represented as a linear combination of two independent sources responsible for the fluctuating Reynolds stresses and the fluctuating enthalpy $\overline{h_t'^2} / h^2$ factor:

$$p = \int G \cdot Q d\mathbf{y} = \int G \cdot Q_1 d\mathbf{y} + \int G \cdot Q_2 d\mathbf{y} \quad F = \iint G(\mathbf{x} | \mathbf{y}_1) G^*(\mathbf{x} | \mathbf{y}_2) Q(\mathbf{y}_1) Q^*(\mathbf{y}_2) d\mathbf{y}_1 d\mathbf{y}_2$$

$$\overline{p^2}(x, r, \omega) = AF_{\text{cold}} + BF_{\text{hot}}$$

Ignore the source directivity + put the sources in the moving frame of the jet

Model 1: the far-field noise spectra formula

$$\overline{p^2}(\mathbf{x}, \mathbf{y}, \omega) = \left[\begin{array}{l} A \cdot [I_{1111} f(\theta, M, \kappa)] + \\ B \cdot [I_{1111} f(\theta, M, \kappa, c, h', \tilde{h})] \end{array} \right] \cdot \frac{\sum_{n=0}^{\infty} (1 + \delta_{n0}) f_n f_n^*}{(1 - M_c \cos \theta)^2}$$

$$I_{1111}(\mathbf{y}, \omega) = C \cdot H(\omega^s \cdot N(kl))$$

Empirical calibration constants: c_l, c_τ and A, B

Model 1: additional approximation

The fluctuation of total enthalpy is not available from RANS solution. So the following empirical model of Khavaran is used:

$$\overline{p^2}(x, r, \omega) = AF_{\text{cold}} + BF_{\text{hot}}$$

$$\frac{\overline{h'_t}}{\tilde{h}} \approx S_T = \left(\left| \frac{dT_t}{dr} \right| \frac{D_j}{T_\infty} \right)^\alpha \frac{(1 - 1/\text{NTR})^\delta}{6} \beta$$

Model 2: final noise prediction formula

The final formula for the acoustic integral:

$$S(\mathbf{x}, \omega) = 4\pi \left(\frac{\pi}{\ln 2} \right)^{\frac{3}{2}} \int_V |p_a(\mathbf{y}, \mathbf{x}, \omega)|^2 \frac{\hat{q}_s^2 l_s^3}{c^2 \tau_s} \frac{\exp \left[-\frac{\omega^2 l_s^2}{\bar{u}^2 (4 \ln 2)} \right]}{1 + \omega^2 \tau_s^2 \left(1 - \frac{\bar{u}}{c_\infty} \cos \varphi \right)^2} d\mathbf{y}$$

The turbulence length and time scales can be determined from RANS similar to Model 1:

$$l_s = c_l \mathbf{K}^{3/2} \varepsilon, \quad \tau_s = c_\tau \mathbf{K} / \varepsilon, \quad \hat{q}_s^2 / c^2 = A^2 (2 / 3 \bar{\rho} \mathbf{K})^2$$

Empirical calibration constants c_l, c_τ and A

Model 3: keeping the realistic source directivity

$$|\hat{p}|^2 = \hat{P}_{\text{Cold}} = \int_V \int_V \hat{R}_{ijkl}(\mathbf{y}, \Delta, \omega) \hat{I}_{ij}(\mathbf{y}, \omega; \mathbf{x}) \hat{I}_{kl}^*(\mathbf{y} + \Delta, \omega; \mathbf{x}) d\Delta d\mathbf{y}$$

where R_{ijkl} is the Fourier transform of the temporal-spatial cross correlation of the turbulent sources:

$$R_{ijkl}(\mathbf{y}, \Delta, \tau) = \overline{T'_{ij}(\mathbf{y}, t) T'_{kl}(\mathbf{y} + \Delta, t + \tau)}$$

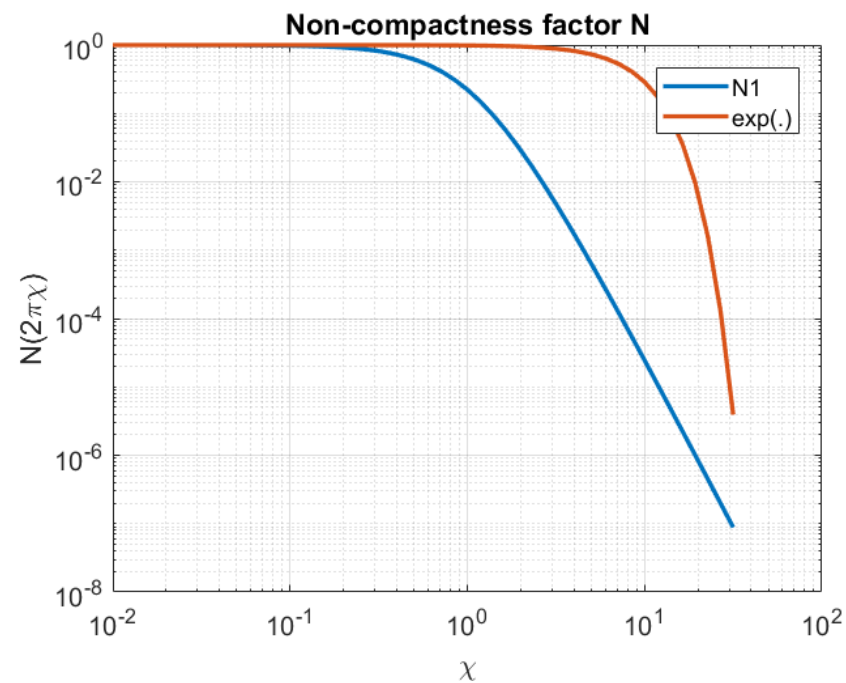
$$T'_{ij} = \rho v_i'' v_j'' - \bar{\rho} v_i'' v_j''$$

Model 3: approximation of the auto-covariance function

We consider Gaussian-exponential model of the auto-correlation function

$$R_{ijkl}(\mathbf{y}, \Delta, \tau) = A_{ijkl}(\mathbf{y}) \exp\left[-\frac{|\Delta_1|}{\tilde{u}\tau_s} - \frac{\ln 2}{l_s^2} \left((\Delta_1 - \tilde{u}\tau)^2 + \Delta_2^2 + \Delta_3^2 \right)\right]$$

The correlation scales are determined from RANS similar to Model 1 and 2, applying the compact scale assumption.



Fluctuating enthalpy model: **NEW!**

To derive the expression for the fluctuating enthalpy term we approximate the auto-covariance of the fluctuating enthalpy stress term,

$$R'_{\text{Hot},j}(\mathbf{y}, \tau) = \overline{T'_{h,i}(\mathbf{y}, t) T'_{h,j}(\mathbf{y} + \Delta, t + \tau)} \quad \text{where} \quad T'_{h,j} = \rho v''_j h''_0 - \bar{\rho} v''_j h''_0$$

(note: $h''_0 \approx h'_t$) by $R'_{\text{Hot},ij}(\mathbf{y}, \tau) \approx \overline{\rho^2 (h''_0)^2 v''_i(\mathbf{y}, t) v''_j(\mathbf{y} + \Delta, t + \tau)}$ **The idea**

Thus, similar to fluctuating Reynolds stress term

$$\overline{v''_i(\mathbf{y}, t) v''_j(\mathbf{y} + \Delta, t + \tau)} \sim D_{ij}(\mathbf{y}) \exp\left[-\frac{|\Delta_1|}{\tilde{u}\tau_s} - \frac{\ln 2}{l_s^2} \left((\Delta_1 - \tilde{u}\tau_s)^2 + \Delta_2^2 + \Delta_3^2\right)\right]$$